2022 19th International Conference on Electrical Engineering, Computing Science and Automatic Control (CCE) Mexico City, Mexico. November 9-11, 2022

# Adaptive Backstepping Control for the Longitudinal Flight of a Blended Wing Body Aircraft

G.A.S. Contreras-Torres
*Postgraduate Program in Aerospace Engineering*
*UPMH, Mexico*
203220016@upmh.edu.mx

R. Garcia-Rodriguez
*Postgraduate Program in Aerospace Engineering*
*UPMH, Mexico*
rogarcia@upmh.edu.mx

C.R. Dominguez-Mayorga
*Postgraduate Program in Aerospace Engineering*
*UPMH, Mexico*
cdominguez@upmh.edu.mx

E. S. Espinoza
*UMI-LAFMIA*
*CINVESTAV*
*CONACYT, Mexico*
eduardo.espinoza@cinvestav.mx

***Abstract*—In recent years, many companies and research groups have been developing the design and control of Blended Wing Body aircraft. Although commercial flights are unavailable today, the first flight is expected in the upcoming years. The Blended Wing Body configuration incorporates many advantages in security, maneuverability, fuel economy, and internal payload, to mention a few. This paper presents the aerodynamic design and control of the Mexican Blended Wing-Body aircraft, EHEKATL. The aerodynamic coefficients are obtained using XFLR5 for a specific flight condition to guarantee static longitudinal stability. Assuming that some aerodynamics coefficients and parameters of the EHEKATL BWB are unknown, an adaptive Backstepping controller for cruise flight is proposed. Stability conditions to guarantee asymptotically convergence of tracking errors are shown. Finally, numerical simulation results, under many conditions, show the satisfactory performance of the proposed approach during cruise phase flight.**

***Index Terms*—Blended Wing-Body Aircraft (BWB), Adaptive Backstepping Controller, Cruise phase flight.**

## I. Introduction

From the Dennis Bushell proposal to McDonnell Douglas, now Boeing, about a new long-range transport aircraft in 1988, the leading manufacturing companies like Boeing and Airbus have been researching and developing new aircraft, such as the X-48 and the MAVERIC, respectively. It was the beginning of the notable effort in the following decades to design, develop, and test flight of the called Blended Wing-Body (BWB) aircraft [1]. As a result of these advances, many aircraft models, such as VELA BWB, NACRE BWB, SAX-40 BWB, and ACFA BWB, have been built and tested in the wind tunnel and flight tests [2], [3].

The BWB is a remarkable aircraft because its shape can increase the capacity for long-range flights or implement a distributed propulsion system offering a wide range of possible configurations and engine sizes, [4]. In addition, BWB aircraft is distinguished by its harmonious fuselage-wing join. Furthermore, whereas the BWB looks like a flying wing, it concentrates a primary payload volume in its central section at first sight. Finally, the BWB is designed as a zero-emission aircraft, that is, to use alternative energy sources, such as electric batteries or hydrogen cells. The advantages of the BWB in comparison with a Tube And Wing (TAW) configuration are due to the minor total wetted area at the same volumetric payload capacity; less parasite drag production thanks to its harmonious fuselage-wing join, and more lift production due to its total lift surface, obtaining an excellent Lift/Drag improvement.

On the other hand, the BWB aircraft represents a challenge in many areas as aerodynamic stability and control. Regarding the control of the aircraft, in contrast with the TAW, the BWB has no empennage where the elevator and rudder usually are located. So, the elevators are relocated in the trailing ledge, and rudders could be in the central body vertical stabilizers or winglets. The issue with locating elevators on the trailing edge is that the arm moment is too short compared with the elevator located in an empennage. In addition, this relocation requires a larger deflection range of the Aerodynamic Control Surface (ACS) to avoid a lack of power [5]. Allocating two or more elevators or ailerons on the trailing edge is common in flying wings or BWBs to produce a bigger control capacity. The distribution of the control surfaces in a BWB aircraft allows control allocation methods to improve the ability to handle failures. In addition, the control allocation can efficiently identify and select the most suitable control surface to complete the task. Thus, the hardware redundancy, the aircraft weight, and the total aircraft cost are some of the main advantages of this configuration [6].

This paper presents a preliminary aerodynamic design and control of the Mexican BWB: EHEKATL[1]. Unlike [7] and [8], the EHEKATL BWB comprises two elevators, two ailerons, and one rudder, see Fig. 1. For the design of the EHEKATL BWB, suitable airfoils for the central body and out wing were selected. Aerodynamic data was obtained with XFLR5

[1]Wind in Nahuatl. The main gods of creation and heroes.

978-1-6654-5508-4/22/$31.00 ©2022 IEEE

according to the EHEKATL BWB geometry and constant airflow conditions, delivering stability and control derivatives essentials to the controller design. Furthermore, it allowed us to carry out static longitudinal analysis to guarantee the EHEKATL BWB capacity to fly and stabilize in the pitching moment. Finally, assuming some aerodynamic coefficients and

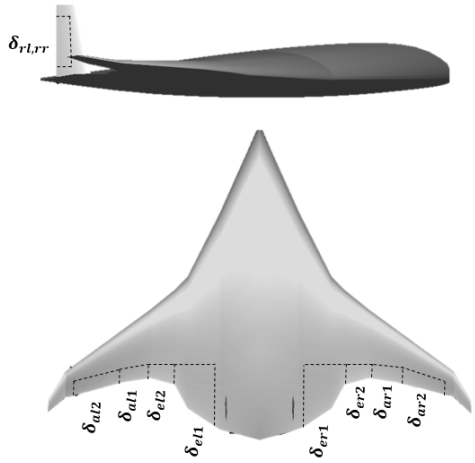


Fig. 1: EHEKATL BWB design and its aerodynamic control surfaces.

parameters are unknown, an adaptive backstepping controller for the EHEKATL BWB in cruise flight is proposed. Thus, asymptotically convergence is guaranteed by using Lyapunov stability.

The remaining of this paper is organized as follows. Section II shows the dynamic flight model of BWB and the longitudinal dynamics for cruise flight. An Adaptive Backstepping controller for BWB in cruise flight is presented in Section III. In the first part of Section IV, the Mexican EHEKATL BWB aerodynamics design is presented, where aerodynamic dimensional stability and control parameters are obtained. In the second part, numerical simulations of the EHEKATL BWB for cruise flights are carried out. Some conclusions and future work are presented in Section V.

## II. BWB Dynamic Model

Using the second law of Newton and assuming that: i) the Earth is flat and approximates to an inertial reference frame, ii) the gravity force is considered constant and perpendicular to the surface of Earth, iii) the aircraft has a plane of symmetry, and iv) the aircraft mass remains constant [9], the EHEKATL BWB equations of motion are given by:

*Translational Motion*

$$\left.\begin{aligned} F_x &= m(\dot{U} + QW - RV) \\ F_y &= m(\dot{V} + RU - PW) \\ F_z &= m(\dot{W} + PV - QU) \end{aligned}\right\} \quad (1)$$

*Rotational Motion*

$$\left.\begin{aligned} M_x &= \dot{P}I_x + QR(I_z - I_y) - (\dot{R} + PQ)I_{xz} \\ M_y &= \dot{P}I_y - PR(I_z - I_x) - (P^2 - R^2)I_{xz} \\ M_z &= \dot{R}I_z + PQ(I_y - I_x) - (QR + \dot{P})I_{xz} \end{aligned}\right\} \quad (2)$$

where $m$ is the mass of the aircraft, $V_b = [U, V, W]^T$ is the linear velocity vector in the body reference frame, $\omega = [P, Q, R]^T$ is the angular velocity vector, and $I_{ij}$ are components of the inertia tensor of the aircraft. Additionally,

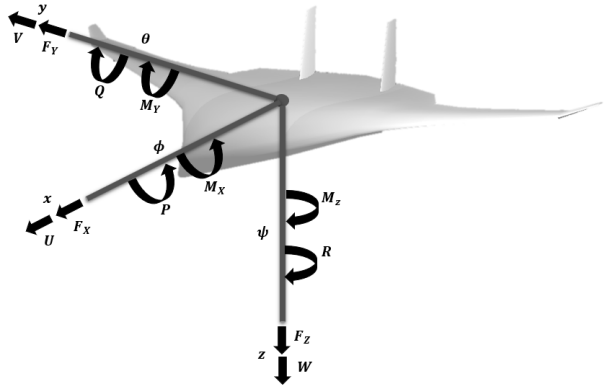


Fig. 2: Principal forces and moments on EHEKATL BWB.

the aircraft forces $F_*$ and moments $M_*$ acting on $x_b$, $y_b$, and $z_b$ axes are defined as $F_x = F_{Ax} + F_{Cx} + F_{Px} + F_{Gx}$, $F_y = F_{Ay} + F_{Cy} + F_{Py} + F_{Gy}$, $F_z = F_{Az} + F_{Cz} + F_{Pz} + F_{Gz}$, and $M_x = M_{Ax} + M_{Cx} + M_{Px}$, $M_y = M_{Ay} + M_{Cy} + M_{Py}$, $M_z = M_{Az} + M_{Cz} + M_{Pz}$, respectively, where A corresponds to aerodynamic components, C the control surfaces, P propulsion components, and G the Earth's gravity. The vector gravity is defined as $F_G = [F_{Gx}, F_{Gy}, F_{Gz}]^T = [-mgS_\theta, mgC_\theta S_\phi, mgC_\theta C_\phi]^T$, and $F_P = [P_T C_\theta C_\psi, P_T S_\psi, P_T C_\psi S_\theta]^T$ represents the propulsion vector with $P_T$ the thrust, assumed constant, and $\theta$, $\psi$ and $\phi$ are the the roll, pitch and yaw angles, respectively [2]. The control surfaces for the EHEKATL BWB are composed by two elevators, $\delta_{eij}$, two ailerons, $\delta_{aij}$, and one rudder, $\delta r$ for $i = l, r$, $j = 1, 2$, see Fig. 1, such that: $F_{Cx} = \sum_{i=1}^{2} X_{\delta_{e_i}}\delta_{e_i}$, $F_{Cy} = \sum_{i=1}^{2} Y_{\delta_{a_i}}\delta_{a_i} + Y_{\delta_r}\delta_r$, $F_{Cz} = \sum_{i=1}^{2} Z_{\delta_{e_i}}\delta_{e_i}$, $L_{Cx} = \sum_{i=1}^{2} L_{\delta_{a_i}}\delta_{a_i} + L_{\delta_r}\delta_r$, $M_{Cy} = \sum_{i=1}^{2} M_{\delta_{e_i}}\delta_{e_i}$, $M_{Cz} = \sum_{i=1}^{2} N_{\delta_{a_i}}\delta_{a_i} + N_{\delta_r}\delta_r$, where $X_{\delta_e}$, $Y_{\delta_{a,r}}$, $Z_{\delta_e}$ are the control force dimensional coefficients, $L_{\delta_{a,r}}$, $M_{\delta_e}$, $N_{\delta_{a,r}}$ are the control moment dimensional coefficients and $\delta_e$, $\delta_a$, $\delta_r$ represent the control surfaces given by the elevators, the ailerons and the rudders, respectively.

### A. Aerodynamics Forces and Moments

The aerodynamic forces and moments are related to the wing aircraft interaction, which in some missions can be related to the Earth's movement. The aerodynamic forces and

[2]For simplicity, it is considered that $\cos(*) = C_*$, and $\sin(*) = S_*$.

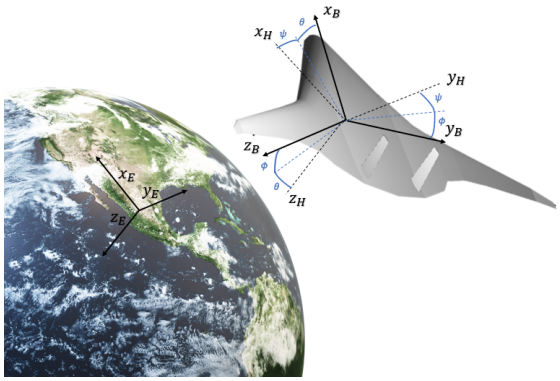


Fig. 3: Principal aircraft reference frames: Earth, Horizontal local plane, and Body.

moments are defined as:

$$\begin{aligned}
F_{Ax} &= \bar{q}SC_D(\alpha, Mach, Re, U, W, Q, \delta_e, \delta_T) \\
F_{Ay} &= \bar{q}SC_Y(\beta, Mach, Re, V, P, R, \delta_a, \delta_r, \delta_T) \\
F_{Az} &= \bar{q}SC_L(\alpha, Mach, Re, U, W, Q, \delta_e, \delta_T) \\
M_{Ax} &= \bar{q}SbC_l(\beta, Mach, Re, V, P, R, \delta_a, \delta_r, \delta_T) \\
M_{Ay} &= \bar{q}ScC_m(\alpha, Mach, Re, U, W, Q, \delta_e, \delta_T) \\
M_{Az} &= \bar{q}SbC_n(\beta, Mach, Re, V, P, R, \delta_a, \delta_r, \delta_T)
\end{aligned}$$

where $\bar{q} = \frac{1}{2}\rho V_w^2$ is the dynamic pressure with $\rho$ the air density and $V_w$ the airspeed; $Mach$ is the Mach number that represents the relationship between aircraft speed and sound speed, and $Re$ is the Reynolds number which characterizes airflow properties as laminar and turbulent flow and is in the function of airfoil chord. $C_D, C_Y, C_L, C_l, C_m, C_n$ are the non-dimensional aerodynamic coefficients of the forces (drag, side force, lift) and moments (roll, pitch, yaw) related to air properties and to the geometry of the airfoil (span $b$, chord $c$, reference area $S$).

Finally, assuming that the airplane rotational rates are small and that the control surface deflections do not affect the forces in the translation equations [9], the rotational kinematics equations are defined as:

$$\begin{bmatrix} \dot{\phi} \\ \dot{\theta} \\ \dot{\psi} \end{bmatrix} = \frac{1}{\cos\theta} \begin{bmatrix} \cos\theta & \sin\phi\sin\theta & \cos\phi\sin\theta \\ 0 & \cos\phi\cos\theta & -\sin\phi\cos\theta \\ 0 & \sin\phi & cos\phi \end{bmatrix} \begin{bmatrix} P \\ Q \\ R \end{bmatrix} \quad (3)$$

For horizontal flight, we will assume that the linear velocity $P$ and the angular velocity $R$ are zero, and the roll and pitch angles are small, such that they can be considered as $\phi = \psi \approx 0$. Thus, the equation (1)-(2) can be rewritten as:

$$\begin{aligned}
F_x &= m(\dot{U} + QW) \quad (4) \\
F_z &= m(\dot{W} - QU) \\
M_y &= \dot{Q}I_y \\
\dot{\theta} &= Q
\end{aligned}$$

The set of equations (4) is also known as the longitudinal dynamics composed of axial velocity U, normal velocity W, and pitch angular velocity $q$. Now, we proceed to design a controller for the *EHEKATL* BWB.

## III. Adaptive Backstepping Controller Design

To control the flight of the BWB in the horizontal plane the elevators $\delta_{eli}$ and $\delta_{eri}$, for $i = 1, 2$, are used, which are moving in the same magnitude and direction, i.e. $\delta_e = \delta_{eli} = \delta_{eri}$, see Fig 1. This is the most straightforward first approach to control the ACS according to the data obtained from XFLR5. We can calculate the control dimensional aerodynamic parameters but consider both or any number of control inputs (two elevators in this case) as one. The other two control inputs on the trailing edge, which corresponds to the ailerons together with the rudders, are not considered to deflect in this paper. By expressing (4) in a state-space representation and including the actuator dynamics as a first-order delay [10], we have:

$$\dot{x} = f(x) + g(x)u_d \quad (5)$$

$$\dot{u} = \frac{1}{\tau}(u_c - u) \quad (6)$$

where $x = [U, W, Q, \theta]^T$ with $\theta$ the uncontrolled state, $\tau$ is a constant time, $u$ is the control signal from the actuator dynamics, $u_c$ is a control command generated by the controller,

$$f(x) = \begin{bmatrix} \frac{1}{m}(F_{Ax} + F_{Px} + F_{Gx}) - QW \\ \frac{1}{m}(F_{Az} + F_{Pz} + F_{Gz}) + QU \\ \frac{1}{I_y}M_{Ay} \\ Q \end{bmatrix},$$

and

$$g(x) = \begin{bmatrix} \frac{1}{m}\sum_{i=1}^{2} X_{\delta_{e_i}} \\ \frac{1}{m}\sum_{i=1}^{2} Z_{\delta_{e_i}} \\ \frac{1}{I_y}\sum_{i=1}^{2} M_{\delta_{e_i}} \\ 0 \end{bmatrix}$$

It is important to notice that the control signal in (5) represents the reference command input, $u_d = \delta_e$.

**Proposition**: Consider that function $f(x) = \varphi^T\eta$ in (5) is unknown, and that the actuator dynamics (6) is included in the BWB longitudinal dynamics. Then, an asymptotically convergence in closed loop is guarantee with the adaptive law $\dot{\hat{\eta}}$, the control command $u_c$ and the reference command $u_d$ given as

$$\dot{\hat{\eta}} = -\Gamma_1^{-1}\varphi z \quad (7)$$

$$u_d = \frac{1}{g(x)}[-\hat{f} + \dot{x}_d - k_z z] \quad (8)$$

$$u_c = u + \tau[\dot{u}_d - k_u z_u] \quad (9)$$

where $k_z$, $k_u$ represent the feedback gains, $\Gamma_1$ is a definite positive matrix, $x_d$ is the reference tracking signal, $z = x - x_d$ represents the longitudinal tracking error, $z_u = u - u_d$ is the control tracking error, $\hat{f} = \varphi^T\hat{\eta}$, and $\tilde{\eta} = \eta - \hat{\eta}$ represents the estimation error with $\hat{\eta}$ being the estimation of unknown parameter vector, and $\varphi(.)$ the smooth nonlinear function.

**Proof** Let a candidate Lyapunov function $V$ be defined as:

$$V = \frac{1}{2}z^T z + \frac{1}{2}z_u^T z_u + \frac{1}{2}\tilde{\eta}^T \Gamma_1 \tilde{\eta} \tag{10}$$

The total derivative of the Lyapunov function along the system trajectories leads to:

$$\begin{aligned}\dot{V} &= z^T \dot{z} + z_u^T \dot{z}_u + \tilde{\eta}^T \Gamma_1 \dot{\tilde{\eta}} \\ &= z^T(\dot{x} - \dot{x}_d) + z_u^T(\dot{u} - \dot{u}_d) + \tilde{\eta}^T \Gamma_1 \dot{\tilde{\eta}} \\ &= z^T(f + g(x)u_d - \dot{x}_d) + z_u^T(\frac{1}{\tau}(u_c - u) - \dot{u}_d) \\ &+ \tilde{\eta}^T \Gamma_1 \dot{\tilde{\eta}} \end{aligned} \tag{11}$$

Substituting (7)-(9) in (11) we have that

$$\dot{V} = -z^T k_z z - z_u^T k_u z_u \leq 0 \tag{12}$$

thus, from the LaSalle-Yoshizawa theorem, the states $z$ and $z_u$ converge asymptotically to the origin as $t \to \infty$. That is, $z = z_u \to 0$ which implies that $x \to x_d$ and $u \to u_d$. In addition from (12) we have that $z, z_u \in L_2$. ■

**Remark.** To simulate the complete system is necessary to consider the following equations

$$\begin{aligned}\dot{z} &= U\theta - W \\ \dot{x} &= UC_\theta + WS_\theta \\ \gamma &= \theta - \alpha \end{aligned} \tag{13}$$

where axial $x$ and $z$ are the axial and normal positions, respectively, with $\gamma$ the path angle trajectory as the input variable and the angle of attack $\alpha = W/V_w$ for small angles, see Fig. 4.

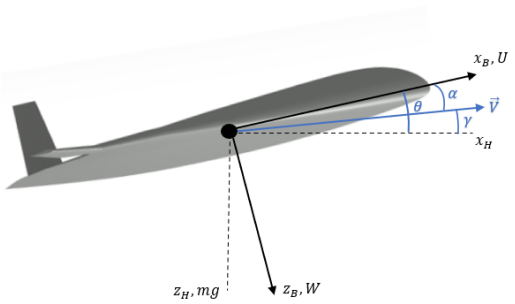


Fig. 4: Flight path angle, pitch angle and angle of attack.

The flight path angle $\gamma$ is the difference between the aircraft velocity vector $\vec{V}$ and the Horizon $x_H$.

## IV. Numerical Results

Before designing a controller, obtaining the aerodynamic coefficients of the stability and control variables is necessary to control the aircraft. These parameters are commonly calculated for a specific flight condition, and even with this consideration, some of them are difficult to calculate accurately. Moreover, flight conditions can change every instant, which results in complex aerodynamic data. For this reason, a robust controller able to adapt online is needed.

### A. Aerodynamic Design

For the preliminary aerodynamics design, EHEKATL BWB airfoils are MARSKE PIONEER IA, which spans from the root chord to the first elevator, and MH 78 14.47 %, which spans from after the first elevator until the tip wing. Vertical stabilizers are with a NACA 0009 Symmetric airfoil. The parameters design used on the CAD scale model are: wing span $b$, wing reference area $S$, aircraft total mass $m$, root chord $l$, mean aerodynamic chord $mac$, center of gravity $cg$, center of pressure $cp$, neutral point $np$, aspect ratio $AR$ and wing loading $w_L$, see TABLE I. The non-dimensional aerodynamic coefficients was calculated using the software XFLR5, as a function of angle of attack, Mach number, and Reynolds number, focusing on longitudinal assumption. see TABLE II.

TABLE I: EHEKATL BWB features and air properties for a flight specific condition

| EHEKATL BWB features and air properties | |
|---|---|
| Geometry Design | Air properties |
| $b = 1.65m$ | $V_w = 12.99\frac{m}{s}$ |
| $S = 0.706m^2$ | $\rho = 1.225\frac{kg}{m^2}$ |
| $m = 2kg$ | $T = 15$ |
| $l = 1.2m$ | $\alpha_e = 3.4$ |
| $mac = 0.695m$ | $40,000 < Re$ |
| $cg = 0.623m$ | $Re < 959,000$ |
| $cp = 0.675m$ | $c = 0.695m$ |
| $np = 0.693m$ | $Mach = 0.035$ |
| $AR = 3.855$ | |
| $w_L = 2.839\frac{kg}{m^2}$ | |

TABLE II: XFLR5 simulation results: Aerodynamic coefficients

| EHEKATL BWB Aerodynamic coefficients | | |
|---|---|---|
| Non-dimensional | Stability | Control |
| $C_L = 0.229$ | $X_u = -0.027843$ | $X_{\delta_e} = 0.30605$ |
| $C_D = 0.015$ | $X_w = 0.34641$ | $Z_{\delta_e} = -8.8438$ |
| $C_m = -0.019$ | $Z_u = -1.5092$ | $M_{\delta_e} = -2.3445$ |
| $CL/CD = 14.79$ | $Z_w = -17.434$ | |
| Efficiency =1.045 | $Z_q = -5.415$ | |
| | $M_u = 6.1021e{-}07$ | |
| | $M_w = -1.2103$ | |
| | $M_q = -1.1697$ | |

### B. Longitudinal Static Stability

Longitudinal static stability refers to the $xz$ plane of symmetry and how the aircraft maintain a certain altitude after facing a gust. The aircraft can return to its equilibrium point or trimmed flight after a small perturbation has occurred. Thus, the study of $Cm$ vs. $C_L$ and $Cm$ vs. $\alpha$ are essential in aircraft longitudinal motion, see Fig. 5. Notice that the aircraft's guarantee the fly capability if $C_m = 0$, and $C_L > 0$. In this case, as analysis results we have that $C_m = 0$, and $C_L = 0.22$, see Fig. 5a. At the same time, notice from Fig. 5b that when $C_m = 0$ the angle of attack is $3.4$ meaning that the trimmed flight is maintaining the initial constant speed $V$ and trimmed angle of attack $\alpha_e$.

On the other hand, when $C_m$ has a negative slope, we get a trimmed angle of attack $\alpha_e$ at zero $C_m$. So when

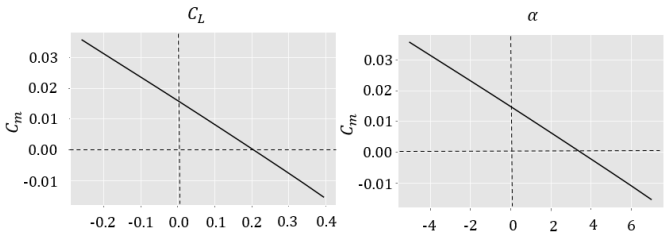


Fig. 5: a) $Cm$ vs. $C_L$, b) $Cm$ vs. $\alpha$

the angle of attack decreases, the aircraft goes nose up, and when $\alpha$ increases, the aircraft goes nose down, restoring trimmed flight for small angles. Thus, the EHEKATL BWB is longitudinal static stable. The constraint longitudinal static stability $M_w, M_q$ are negative, and the speed effects are taken into account and defines a general requirement for longitudinal static stability as $\partial C_m/\partial C_L < 0, \partial C_m/\partial C_\alpha < 0$. Once the aerodynamic design is finished, we show the performance of the proposed approach.

### C. Simulation Results

We conducted numerical simulations on Python with the ANACONDA suite and its free-integrated development environment (IDE): SPYDER. We use three libraries: Numpy for arrays and linear algebra, Odeint from SciPy to integrate and solve ODE, and Matplotlib to plot and visualize the numerical results, showing the proposed approach's performance. We defined two mission profiles: a) in the first mission profile, the aircraft starts climbing until $24m$; next, the controller maintains this altitude for $15s$, then climbs again until almost $50m$. After a while, the aircraft descents to $33m$, and finally, it descents to $7m$ to finish the mission, b) for the second mission profile, we defined a cruise flight when a perturbation occurs. When a gust appears, the aircraft is in a trimmed flight at $59m$ altitude; the altitude descends to $51m$. The controller recovers the altitude after $7s$ and maintains the path trajectory at a constant angle of attack with a smooth and oscillating pitch movement.

For both missions, the feedback control gains, the adaptive gains, and the constant time step were defined as:

$$k_z = \begin{bmatrix} 0.3 & 0 & 0 \\ 0 & 0.9 & 0 \\ 0 & 0 & 0.6 \end{bmatrix}, k_u = \begin{bmatrix} 60 & 0 & 0 \\ 0 & 60 & 0 \\ 0 & 0 & 60 \end{bmatrix}$$
$$\Gamma_1 = \begin{bmatrix} 3 & 0 & 0 \\ 0 & 9 & 0 \\ 0 & 0 & 9 \end{bmatrix}, \tau = 0.03 \quad (14)$$

Two engines produce the thrust that yields $5N$ in total. The main results obtained from both simulation scenarios are summarized as follows:

a) *Mission 1*: Climbing, Cruise, and Descent. Fig. 6 show the output variables and input control signal. In an ordinary flight, an aircraft performs taxi out, take off, climbing, cruise, descent, approximation and landing, and taxi in phases. In

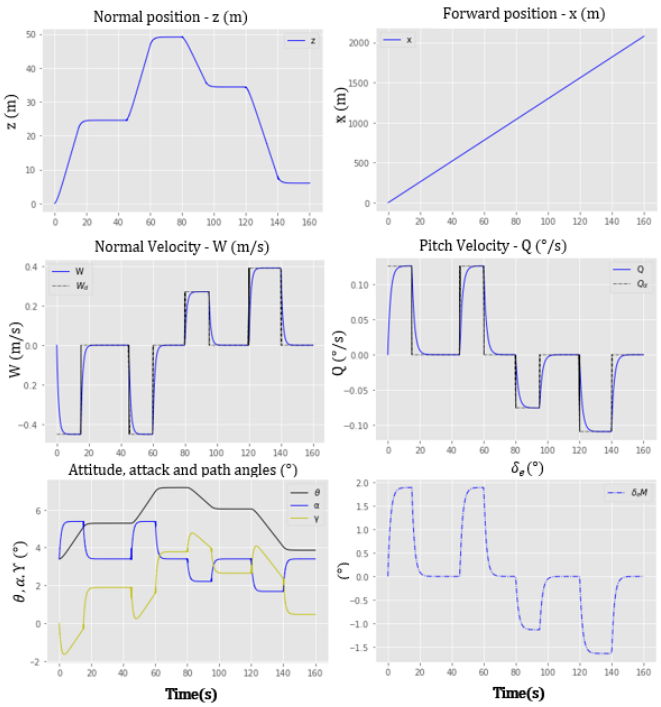


Fig. 6: Mission I: Climbing, Cruise and Descent

this mission, we only considered the climbing, cruise, and descent phases, which is a profile that can be executed at constant velocity. Furthermore, the aircraft altitude refers to the normal position $z$. We control elevator deflection $\delta_e$ to track a certain pitch velocity $Q$, or normal velocity $W$; hence we have an altitude change $z$ at constant speed $V$. The pitch attitude angle $\theta$ spans from the horizontal plane to the aircraft body frame, while the angle of attack $\alpha$ spans from the axial body axes to the airspeed vector. The path trajectory $\gamma$ is the difference between both angles and the actual trajectory the aircraft follows. We notice that as $\theta$ increases, $\alpha$ increases too, but just after, $\alpha$ recovers to $\alpha_e$ thanks to static stability.

b) *Mission II*: Cruise flight - Recovering trim after a gust. Fig. 7 shows the output variables and the input control obtained in this mission profile with white noise. Notice how the white noise affects the pitch $Q$ and normal $W$ velocities. The mission is to keep an altitude of $59m$. The simulation begins with a strong gust, disturbing the aircraft to descend 8m. We can see that the controller recovers the aircraft's fixed altitude after seven seconds, maintaining a constant angle of attack with smooth and oscillating pitch movement. The path angle $\gamma$ keeps close to zero, which means the aircraft's axial longitudinal trajectory follows. This movement change altitude in a few range $59 - 60m$ at $\alpha_e$. The elevator compensates the perturbation with a deflection of $-4$ and keeps the pitch oscillation with a deflection of $+/-1$.

## V. Conclusions

EHEKATL BWB is a novel Mexican design created by the synergy effort of UPMH and CINVESTAV. We expect a zero-

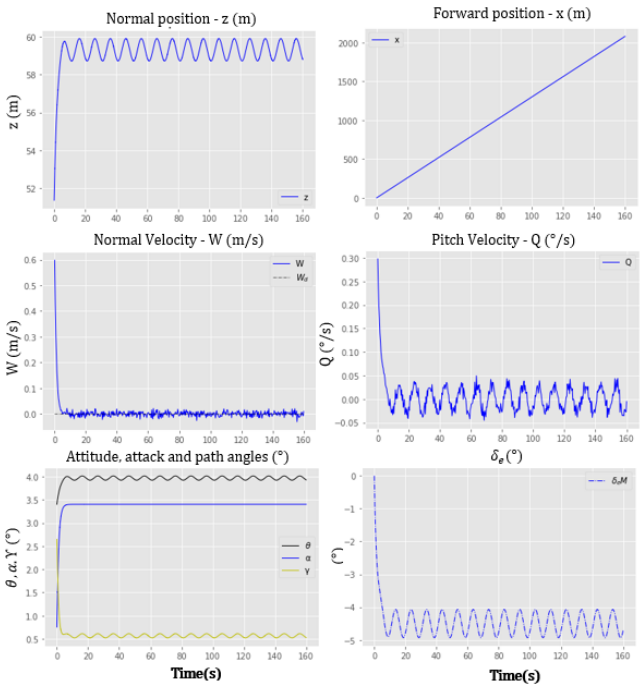


Fig. 7: Mission 2: Cruise flight; recovering trim after a perturbation

emission autonomous logistical aeronautic system for different long-rage and payload freight applications. This work aimed to develop an Adaptive Backstepping control for the longitudinal flight of the EHEKATL BWB aircraft that allows robustness to complete missions I-II with the same control and adaptive gains and assuming unknown parameters in the aerodynamic data. The stability analysis guaranteed the asymptotical convergence of tracking errors with smoother signals related to the established gain vectors. Determining the aerodynamics coefficients is crucial to knowing the aircraft's capabilities, such as flying and static stability, as we demonstrated with three coefficients $C_L, C_m, \alpha$. However, establishing invariant parameters for aircraft controllers is idealistic because actual aircraft functions are variants in time.

Future work will study:

- The control dimensional aerodynamic parameters of every control input on the trailing edge to implement a control allocation scheme together with the adaptive controller.
- The lateral-directional dynamics as the full nonlinear aircraft dynamics 6-DOF.
- The design of neuro-adaptive backstepping controllers.
- The validation of aerodynamic analysis using XFLR5, ANSYS, and Dassault Systems simulations.
- Modelling-In-The-Loop with X-PLANE to finally build the scale model for flight tests with Hardware-In-The-Loop.

.


## ACKNOWLEDGEMENTS

This work was partially supported by CONACYT Master Studies Scholarship No. 1079163 granted to the first author.


## REFERENCES


[1] B. I. Larrimer. *Beyond Tube and Wing*. URL: https://www.nasa.gov/sites/default/files/atoms/files/beyond_tube-and-wing_tagged.pdf. 2020.

[2] M. Zozek and A. Schirrer. *Modeling and Control for a Blended Wing Body Aircraft: A Case Study.* SPRINGER, 2015.

[3] Zhenli C. et al. "Assessment on critical technologies for conceptual design of blended-wing-body civil aircraft". In: *Chinese Journal of Aeronautics* (2019).

[4] P. Kumar and A. Khalid. "Blended Wing Body Propulsion System Design". In: *International Journal of Aviation, Aeronautics, and Aerospace* 4 (2017). DOI: https://doi.org/10.15394/ijaaa.2017.1187.

[5] Honglin C. *Effectiveness of Thrust Vectoring Control for Longitudinal Trim of a Blended Wing Body Aircraft*. URL: https://repository.tudelft.nl/islandora/object/uuid:de4a4261-0948-45e9-9525-b78e2a664af2/datastream/OBJ/download. 2015.

[6] N. Zhang, F. Li, and L. Wang. *Control Allocation Approach Study for BWB Aircraft*. SPRINGER, June 2019, pp. 2099–2115. DOI: 10.1007/978-981-13-3305-7_168.

[7] Weifang S. Shaojie Z. and Qingkai M. "Control Surface Faults Neural Adaptive Compensation Control for Tailless Flying Wing Aircraft with Uncertainties". In: *International Journal of Control, Automation and Systems* 4 (2018). DOI: http://dx.doi.org/10.1007/s12555-017-0454-y.

[8] J. Shi X. Qu. "Reconfigurable Flight Control System Design for Blended Wing Body UAV Based on Control Allocation". In: *International Conference on Control, Automation and Systems (ICCAS)* (2018), pp. 632–638.

[9] B. Etkin. *Dynamics of flight. Stability and control.* WILEY, 1996.

[10] Byunghun C. "Robust Control Allocation with Adaptive Backstepping Flight Control". In: *Journal of Aeropace Engineering* 228(7) 1033 1046 (2013), p. 14. DOI: 10.1177/0954410013483687.